ADDING HARD X-RAY IMAGING CAPABILITIES TO A COMPTON TELESCOPE

Cornelia B. Wunderer[1], **Mark E. Bandstra**[1], **Steven E. Boggs**[1], **Jason D. Bowen**[1], **and Wayne Coburn**[1]

[1]*Space Sciences Laboratory, UC Berkeley, CA 94720, USA*

ABSTRACT

The efficiency of a Compton telescope operating in its "imaging mode" decreases rapidly with energy below a few hundred keV. At the same time, the achievable angular resolution in Compton mode also declines. The efficiency decrease is mainly due to the increasing photoabsorption cross sections at these low energies. The average distance between interaction sites for Compton events decreases with decreasing photon energy; this, together with the increasing impact of Doppler broadening, results in the instrument's angular resolution rapidly deteriorating as the photon energy decreases. These limitations of efficiency and angular resolution constitute essentially "fundamental" limits on the energy regime accessible to imaging Compton telescopes.

At the same time, a Compton Telescope at balloon altitudes or in space is exposed to Cosmic diffuse and atmospheric photon backgrounds. The intensity of both of these components increases rapidly with decreasing energy, making photons $< 100\,\mathrm{keV}$ a possibly significant contributor to random coincident events or instrument dead time. Thus shielding of low-energy photon components is desirable.

For the first balloon flight of the Nuclear Compton Telescope (NCT) we have simultaneously reduced low-energy background and enabled hard X-ray imaging by enshrouding the top of the instrument in a tin shield (bottom had BGO shielding), with part of the shield having strategically placed holes — a 10% open coded aperture mask working up to $\sim 80\,\mathrm{keV}$ in conjunction with the finely pixellated double-sided Ge strip detectors. We present pre-flight calibration results of this coded mask.

Key words: Compton telescope, coded mask, hard X-ray imaging, NCT.

1. INTRODUCTION - THE NUCLEAR COMPTON TELESCOPE

The Nuclear Compton Telescope (NCT, [2]) is a modern Compton Telescope based on cross-strip germanium detectors and represents a promising candidate technology for an Advanced Compton Telescope (ACT, [1, 3, 7]). Fine 3-D interaction positioning together with the fine spectral resolution that only Ge detectors offer at MeV energies enable a compact, high-stopping-power twelve-detector array (see Fig. 1) — providing excellent spectral and good spatial resolution, ideal for nuclear astrophysics.

In each of the NCT detectors, active anode (DC) and cathode (AC) strips give the 2-D interaction positions (see Fig. 2). Timing between anode and cathode strips yields depth information to $\sim 0.4\,\mathrm{mm}$ FWHM. Detailed energy

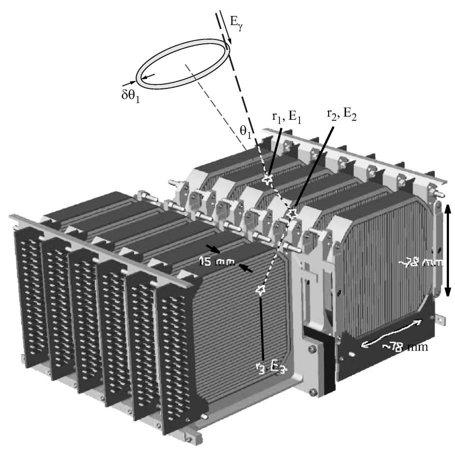

Figure 1. The full NCT detector array. The balloon prototype flown in 2005 only had 2 of the 12 detectors. Multiple-interaction Compton event shown with the corresponding event circle.

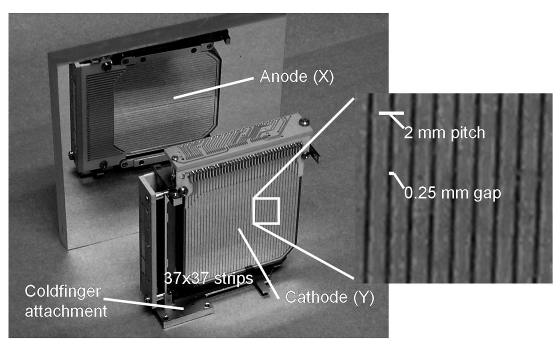

Figure 2. Photograph of a single NCT Ge detector. The cross-strip design enables x and y pixellation with 2 mm pitch.

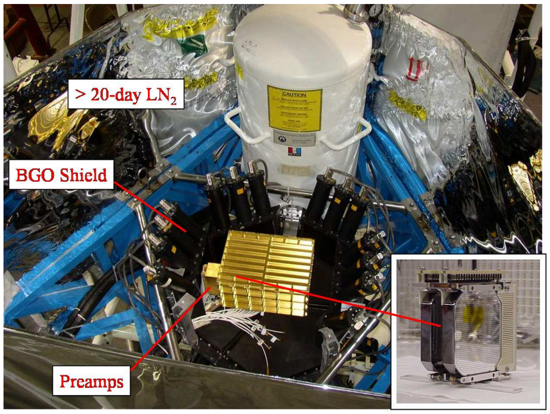

Figure 3. NCT balloon gondola (as flown, except for thermal shielding and tin shield/mask). The NCT cryostat is designed for 12 detectors. During this prototype flight, it contained only two Ge-strip detectors (placed at the front left of the cryostat).

and position calibrations for a two-detector prototype are discussed in [4].

The two-detector prototype instrument flew on a balloon on July 1, 2005, from Ft Sumner, NM. A picture of the NCT gondola is shown in Fig. 3. The NCT instrument worked fine and was recovered in great condition. Unfortunately, the balloon gondola's aspect control failed during the flight. While we do retain knowledge of our pointing, and NCT has a wide field-of-view, this impacts NCT's Compton effective area and significantly complicates data analysis.

This paper focuses on a side aspect of the NCT prototype balloon payload — a low-energy passive shield doubling as a hard X-ray coded aperture.

2. MOTIVATION

2.1. Imaging Hard X-Rays

Compton scattering is the dominant interaction in Ge only well above 100 keV (see Fig. 4). Moreover, distances between two interactions of Compton-scattered $\sim$150 keV photons are most often too short to be separable on scales such as the NCT detector's strip pitch (2 mm). Consequently, interactions of photons below $\sim$200 keV in NCT most often occur as "single-site events" — given the instrument's spatial resolution, no more than one interaction can be recognized. Such "single-site" event data is not useful to the Nuclear Compton Telescope in its primary detection mode.

It is, however, vital to NCT's performance to be able to detect and trigger on individual interactions of tens of keV — multiple such interactions do make up valid Compton events. The NCT prototype detectors trigger on *and record* individual interactions above $\sim$40 keV (above 15 keV with revised electronics). Given the fine pixellation of the detectors and their low single-interaction thresholds, the NCT Ge detectors are well suited as detection plane for a hard X-ray coded mask.

2.2. Shielding for a Compton Telescope

Soft γ-ray photon backgrounds both at balloon altitudes and in space increase rapidly with decreasing photon energy (see Fig. 5). "Unwanted" single-site interactions thus would constitute a significant fraction of NCT events, resulting (a) in a high random coincidence rate and (b) in a significantly larger data volume without the implementation of an on-board coincident trigger requirement.

A 0.25 mm tin shield around the NCT detectors reduces the low-energy photon contribution to the background events below $\sim$100 keV significantly (86% opaque at 50 keV), while not reducing the instrument's efficiency above $\sim$200 keV (94% transparent at 200 keV).

It is possible to achieve both low-energy background reduction *and* hard X-ray imaging at the same time — by surrounding NCT's finely pixellated Ge detectors with a thin tin shield with "a few strategically placed holes": a hard X-ray low-opening-fraction coded mask.

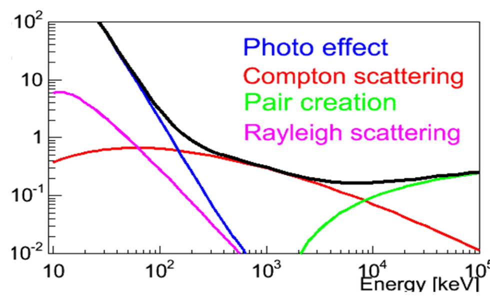

Figure 4. Photon interaction cross sections in Ge.

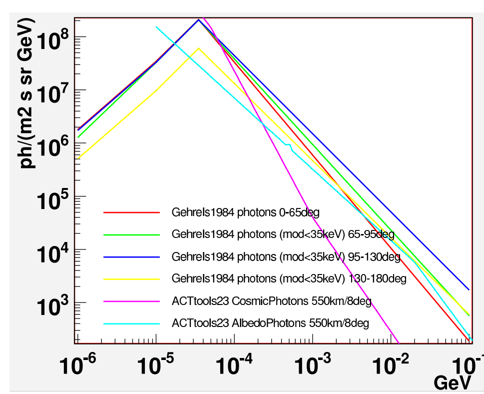

Figure 5. Photon backgrounds at balloon altitudes and in low-earth orbit, taken from [5] and the ACT environment tools (see [1, 6]).

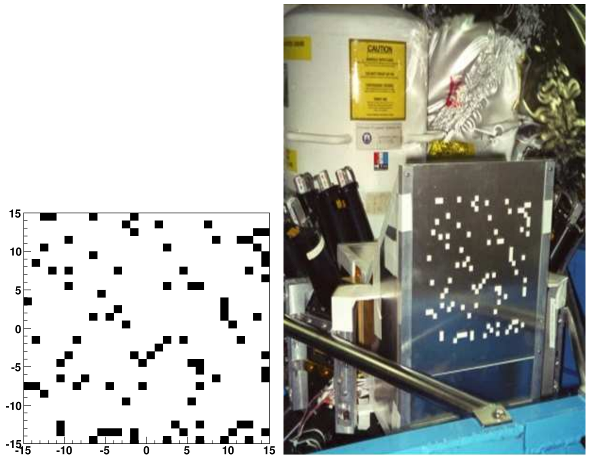

Figure 6. Illustration of NCT mask pattern and photograph of NCT gondola with mask and tin shielding.

3. MASK DESIGN

A good coded mask pattern for the low-energy extension of the NCT prototype balloon payload had to fulfill several requirements:

- low opening fraction to retain the shielding function as a safeguard against high low-energy event data rates and random coincidences
- optimized for point sources (main observation target planned for a 30-hour turnaround flight was the Crab)
- mask element size suitable match for the $2\times2\,\mathrm{mm}^2$ Ge detector pixels
- mounting constraints for the mask dictated a mask-detector distance of $\sim30\,\mathrm{cm}$ and a mask area of about $20\times20\,\mathrm{cm}^2$

The approach we took to designing such a mask was to first decide on a mask open fraction of 10% as a compromise between low enough background rates and high enough Crab flux, and a mask element size of $7\times7\,\mathrm{mm}^2$ in a 30×30 element mask. The mask pattern was then determined by picking the best pattern from a group of 200 randomly generated masks according to a series of criteria outlined below. (Since URA designs exhibit their good autocorrelation function properties only if the mask pattern is repeated at least once, picking a good random mask was preferred over an URA design.)

We generated 200 candidate masks, each with 90 open mask elements (10%). We required that each 7×7 mask element area contains at least one open mask element — to ensure some low-energy photon throughput from a point source at any position within the FoV. We determined autocorrelation functions (ACFs) for each mask separately for each possible point source position within the fully coded field of view, *using only the part of the mask pattern whose shadow would actually be recorded on the detector*. For each mask, we determined the source position with the lowest signal-to-noise ratio according to the ACF — this ratio describes the worst-case performance of that particular mask. Out of the 200 mask patterns, we picked the one with the highest worst-case signal-to-noise ratio. The pattern, along with a photograph of the NCT balloon payload with mask in place, is shown in Fig. 6. The lowest ratio of source peak to highest noise peak in the ACF for the chosen mask is 2.7 (for one particular source position, for all other possible source positions this ratio is higher).

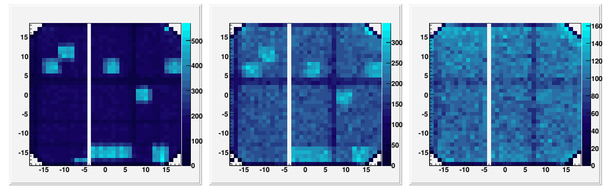

Figure 7. Raw shadowgrams of the mask taken (left to right) in the 60 keV line of $^{241}\mathrm{Am}$*, the 80 keV line of* $^{133}\mathrm{Ba}$*, and the 122 keV line of* $^{57}\mathrm{Co}$*. The white line corresponds to a defective electronics channel.*

4. LABORATORY RESULTS

The NCT cryostat was shielded by solid 0.25 mm tin sheets in all directions not covered by either the mask or the instrument's BGO anticoincidence shield (see Fig. 6).

Raw shadowgrams of the mask in gamma-ray lines at 60 keV ($^{241}\mathrm{Am}$), 80 keV ($^{57}\mathrm{Co}$ and $^{133}\mathrm{Ba}$ combined run), and 122 keV ($^{57}\mathrm{Co}$ and $^{133}\mathrm{Ba}$ combined run) illustrate the rapidly increasing transparency of the tin coded aperture above $\sim100\,\mathrm{keV}$ (Fig. 7). In the raw shadowgrams, besides the pattern generated by the mask, both a defective electronics channel of one strip (white) and shadows of structural support ridges of the cryostat wall are clearly evident. Especially the latter result in additional features in the shadowgram, similar in effect to large pixel-to-pixel variations in detector efficiency. A removal of these cryostat shadows of course enables cleaner shadowgrams and thus better source reconstruction. For the data analysis performed here, we used source data obtained before the mask was mounted to calculate the appropriate intensity corrections. Fig. 8 shows a raw shadowgram of an $^{241}\mathrm{Am}$ source in the 60 keV line, the correction matrix obtained from a measurement without mask taken with the same source, and the renormalized shadowgram. Figs. 9 and 10 finally show images of laboratory $^{241}\mathrm{Am}$ sources obtained using a simple cross-correlation algorithm. The imaging positions are derived using (tape-)measured mask position information. A combination of all available calibration data could be used to derive a corrected mask position.

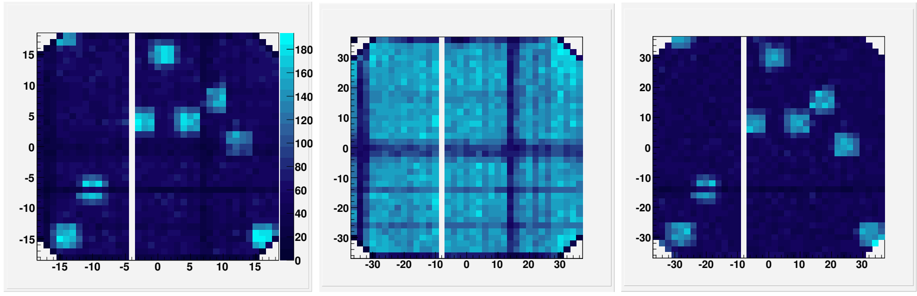

Figure 8. Raw shadowgram (left), correction matrix obtained from measurement without mask (center), and corrected shadowgram (right) in the 60 keV light of an $^{241}\mathrm{Am}$ *laboratory source.*

5. CONCLUSIONS AND OUTLOOK

Due to the late addition of the mask to the balloon payload, the mask position could only be determined using tape measure after it was mounted. The resulting uncertainty in mask-detector distance and mask-detector tilt angle prevents source positioning accuracy to better than $\sim 0.5°$; rotation-induced errors are larger further off mask-detector axis. In principle, the analysis of the shadowgram should also be performed as a function of interaction depth in the detector — again this effect has a larger impact at larger off-axis angles. Even a position accuracy of $\sim 0.5°$ would still have been adequate for a secondary instrument to the Compton imager.

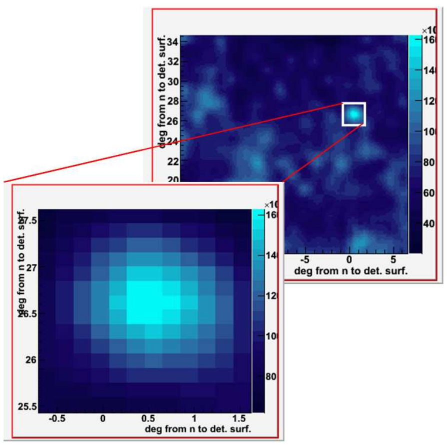

Figure 9. NCT-observed laboratory $^{241}\mathrm{Am}$ *source (60 keV). The true source position was at (1.1°,25.2°). See text.*

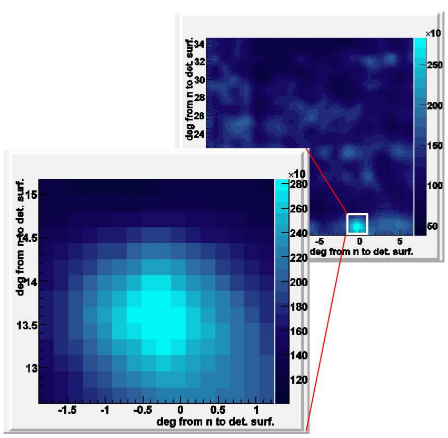

Figure 10. NCT-observed laboratory $^{241}\mathrm{Am}$ *source (60 keV). The true source position was at (-0.1°,13.3°). See text.*

Unfortunately, the aspect system failure of the NCT gondola kept Crab out of the *mask's* FoV for most of the flight.

The NCT team is currently analyzing the prototype flight data, as well as preparing the instrument for a 12-detector long-duration balloon flight which is foreseen from Australia in 2008. We intend to again fly a low-energy coded mask / shield configuration on that instrument.

ACKNOWLEDGMENTS

We thank NASA grant NNG04WC38G for support of the NCT balloon prototype. CBW also thanks the Townes Fellowship at UC Berkeley for support.

REFERENCES

[1] S.E. Boggs et al. ACT Study Report, 2005. available at ”http://ssl.berkeley.edu/act/”.

[2] S.E. Boggs et al. Exp. Ast., 2006. in press.

[3] S.E. Boggs et al. In SPIE Proc. volume 6266, 626624–1. 2006.

[4] J.D. Bowen et al. In SPIE Proc. volume 6266, 626625–1. 2006.

[5] N. Gehrels. *Nucl. Instrum. Methods Phys. Res., Sect. A*, A 239:324–349, 1985.

[6] C.B. Wunderer et al. New Astr. Rev., 2006. in press.

[7] C.B. Wunderer et al. The Advanced Compton Telescope Mission. this volume.